

Axis Tour: Word Tour Determines the Order of Axes in ICA-transformed Embeddings

Hiroaki Yamagiwa¹ Yusuke Takase¹ Hidetoshi Shimodaira^{1,2}
¹Kyoto University ²RIKEN AIP
{hiroaki.yamagiwa, y.takase}@sys.i.kyoto-u.ac.jp,
shimo@i.kyoto-u.ac.jp

Abstract

Word embedding is one of the most important components in natural language processing, but interpreting high-dimensional embeddings remains a challenging problem. To address this problem, Independent Component Analysis (ICA) is identified as an effective solution. ICA-transformed word embeddings reveal interpretable semantic axes; however, the order of these axes are arbitrary. In this study, we focus on this property and propose a novel method, Axis Tour, which optimizes the order of the axes. Inspired by Word Tour, a one-dimensional word embedding method, we aim to improve the clarity of the word embedding space by maximizing the semantic continuity of the axes. Furthermore, we show through experiments on downstream tasks that Axis Tour constructs better low-dimensional embeddings compared to both PCA and ICA.

1 Introduction

Word embedding is one of the most important components in natural language processing, but interpreting high-dimensional embeddings remains a challenging problem. To address this problem, Independent Component Analysis (ICA) (Hyvärinen and Oja, 2000) is identified as an effective solution (Mareček et al., 2020; Musil and Mareček, 2022; Yamagiwa et al., 2023). ICA-transformed word embeddings reveal interpretable semantic axes; however, the order of these axes are arbitrary (Hyvärinen et al., 2001b).

Inspired by a one-dimensional word embeddings, Word Tour (Sato, 2022), which leverages the Traveling Salesman Problem (TSP), we aim to improve the clarity of the word embedding space by maximizing the semantic continuity of the axes.

Fig. 1 shows two sets of two-dimensional projections of word embeddings: one set is ordered by Axis Tour and the other is sorted in descending order of skewness (Skewness Sort). In Axis Tour, the most significant words of the axes are far from

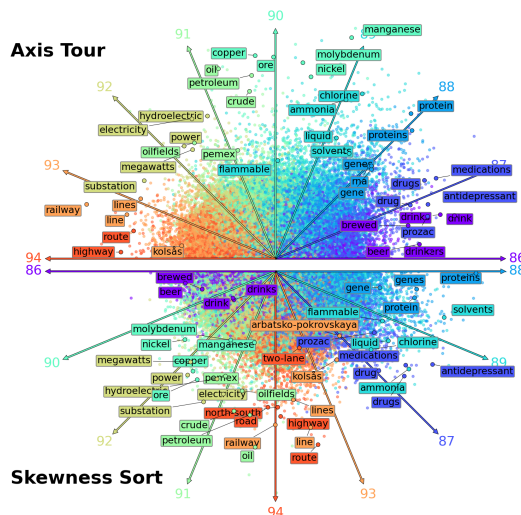


Figure 1: Scatterplots of normalized ICA-transformed word embeddings whose axes are ordered by Axis Tour and Skewness Sort. In the upper part, Axis Tour is applied to 300-dimensional GloVe, with nine consecutive axes arranged counterclockwise. In the lower part, these nine axes are arranged clockwise in descending order of skewness. The embeddings are projected onto two dimensions along these axes. The top five embeddings on each axis are labeled by their words. Each word is assigned the color of the axis with the highest value. In both cases, words that cross the horizontal axes are not displayed.

the center, with the meanings of the axes changing continuously. Conversely, in Skewness Sort, the most significant words are nearer to the center, and axes with different meanings are placed adjacently. In fact, the average distance from the origin to these significant words in Fig. 1 is 0.76 in Axis Tour, as opposed to 0.65 in Skewness Sort.

We also assume that the consecutive axes in the Axis Tour embeddings can be considered as a subspace whose axes have similar meanings. Based on this, we project each subspace onto a single dimension to achieve dimensionality reduction. We show through experiments that Axis Tour yields better

low-dimensional embeddings when compared to both PCA and ICA.

2 Related work

There are studies that transform embeddings by rotation (Park et al., 2017) from Factor Analysis (Crawford and Ferguson, 1970; Browne, 2001) or Principal Component Analysis (PCA) (Musil, 2019). Independent Component Analysis (ICA) (Hyvärinen and Oja, 2000) has gained attention for its ability to reveal interpretable semantic axes in the transformed embeddings (Mareček et al., 2020; Musil and Mareček, 2022; Yamagiwa et al., 2023).

Relevant for our study is Topographic ICA (TICA) (Kohonen, 2001; Hyvärinen et al., 2001a). TICA relaxes the assumption of statistical independence and assumes energy correlations between adjacent axes. TICA then estimates the order of the axes. Unlike TICA, Axis Tour applies to ordinary ICA-transformed embeddings and uses the embeddings themselves to measure axis similarity.

3 Background

The pre-trained word embedding matrix is given by $\mathbf{X} = [\mathbf{x}_1, \dots, \mathbf{x}_n]^\top \in \mathbb{R}^{n \times d}$, where \mathbf{X} is *centered* (i.e., the mean of each column is zero). Here, $\mathbf{x}_i \in \mathbb{R}^d$ represents the word embedding of the i -th word.

3.1 ICA-transformed word embeddings

ICA (Hyvärinen and Oja, 2000) finds the transformation matrix $\mathbf{B} \in \mathbb{R}^{d \times d}$ such that the columns of the matrix $\mathbf{S} \in \mathbb{R}^{n \times d}$, represented by the following equation, are as statistically independent as possible:

$$\mathbf{S} = \mathbf{XB}, \quad (1)$$

where \mathbf{S} is assumed to be *whitened* (i.e., the variance of each column is 1). The columns of \mathbf{S} are called independent components¹.

While the matrix \mathbf{S} has interpretable semantic axes (Mareček et al., 2020; Musil and Mareček, 2022; Yamagiwa et al., 2023), the order of these axes are arbitrary (Hyvärinen et al., 2001b).

3.2 Word Tour

Let $\mathcal{P}([n])$ be the set of all permutations of $[n]$, where $[n] = \{1, \dots, n\}$. Word Tour (Sato, 2022) is a one-dimensional word embeddings method

¹Unless otherwise noted, flip the sign of each axis as needed so that the skewness is positive.

which solves the following Traveling Salesman Problem (TSP):

$$\min_{\sigma \in \mathcal{P}([n])} \|\mathbf{x}_{\sigma_1} - \mathbf{x}_{\sigma_n}\| + \sum_{i=1}^{n-1} \|\mathbf{x}_{\sigma_i} - \mathbf{x}_{\sigma_{i+1}}\|. \quad (2)$$

The resulting one-dimensional embeddings have similar meanings if they are close in order.

4 Axis Tour

This section explains Axis Tour and the dimensionality reduction method using Axis Tour. As mentioned in Section 3.2, $[d] = \{1, \dots, d\}$ and $\mathcal{P}([d])$ is the set of all permutations of $[d]$.

4.1 Definition of axis embedding

We define *axis embedding* for use in Word Tour. The embedding represents the axis of the ICA-transformed embeddings \mathbf{S} .

In preparation, we define the matrix $\hat{\mathbf{S}} \in \mathbb{R}^{n \times d}$ as the normalization of the embeddings \mathbf{S} with row vectors $\hat{\mathbf{s}}_i = \mathbf{s}_i / \|\mathbf{s}_i\|$. Here, the i -th word embedding of \mathbf{S} and $\hat{\mathbf{S}}$ are denoted by $\mathbf{s}_i, \hat{\mathbf{s}}_i \in \mathbb{R}^d$, respectively. We compare the elements of the ℓ -th axis of $\hat{\mathbf{S}}$ and denote the index set of words corresponding to the top k elements as Top_k^ℓ .

We then define the ℓ -th axis embedding \mathbf{v}_ℓ for \mathbf{S} as follows:

$$\mathbf{v}_\ell := \frac{1}{k} \sum_{i \in \text{Top}_k^\ell} \hat{\mathbf{s}}_i \in \mathbb{R}^d. \quad (3)$$

As we saw in Fig. 1, since the meaning of an axis can be interpreted from the top words, \mathbf{v}_ℓ can be considered as the embedding that represents the meaning of the ℓ -th axis of \mathbf{S} .

4.2 Determining the order of axes

Axis Tour is a method that uses \mathbf{v}_ℓ in (3) to perform Word Tour and determines the order of axes in ICA-transformed word embeddings. In Axis Tour, the cost between the axis embeddings $\mathbf{v}_\ell, \mathbf{v}_m$ used for TSP is defined by $1 - \cos(\mathbf{v}_\ell, \mathbf{v}_m)$ instead of $\|\mathbf{v}_\ell - \mathbf{v}_m\|$. This approach then maximizes the sum of cosine similarities between adjacent axis embeddings. Therefore, the problem is formulated as follows²:

$$\max_{\tau \in \mathcal{P}([d])} \cos(\mathbf{v}_{\tau_1}, \mathbf{v}_{\tau_d}) + \sum_{\ell=1}^{d-1} \cos(\mathbf{v}_{\tau_\ell}, \mathbf{v}_{\tau_{\ell+1}}). \quad (4)$$

²Note that due to the cyclic nature of τ , we ensure that $\cos(\mathbf{v}_{\tau_1}, \mathbf{v}_{\tau_d})$ is the smallest of the cosine similarities.

The sum of cosine similarities between adjacent axis embeddings can be considered as a measure of the semantic continuity of the axes. Thus, Axis Tour determines the order of the axes by maximizing this measure.

4.3 Dimensionality reduction

Let $\mathbf{T} = [t_1, \dots, t_n]^T \in \mathbb{R}^{n \times d}$ be the matrix \mathbf{S} with Axis Tour applied. We consider reducing the dimensions from d to $p (\leq d)$ by merging the consecutive axes of \mathbf{T} . In preparation, we divide $[d]$ into p equal-length intervals³ and define the index set for the r -th interval as $I_r := \{a_r, \dots, b_r\}$ ($a_r, b_r \in [d], a_r \leq b_r$). Let $\gamma_\ell \in \mathbb{R}_{\geq 0}$ be the skewness of the ℓ -th axis of \mathbf{T} ⁴.

First, we consider dimensionality reduction for I_r . To do this, we define a vector $\mathbf{f}_r = (f_r^{(\ell)})_{\ell=1}^d \in \mathbb{R}_{\geq 0}^d$ of length 1 for each I_r as follows:

$$f_r^{(\ell)} = \begin{cases} \gamma_\ell^\alpha / \sqrt{\sum_{m=a_r}^{b_r} \gamma_m^{2\alpha}} & \text{for } \ell \in I_r \\ 0 & \text{otherwise,} \end{cases} \quad (5)$$

where $\alpha \in \mathbb{R}_{\geq 0}$. Then $\mathbf{T}\mathbf{f}_r \in \mathbb{R}^n$ can be considered as a projection of the subspace spanned by the axes of \mathbf{T} corresponding to I_r onto a one-dimensional space. Fig. 5 in Appendix A shows the projection for three consecutive axes.

Next, we define the matrix $\mathbf{F} := [\mathbf{f}_1, \dots, \mathbf{f}_p] \in \mathbb{R}^{d \times p}$. Then $\mathbf{TF} \in \mathbb{R}^{n \times p}$ represents the concatenated projections, that is, a dimensionality reduction of the d -dimensional embeddings \mathbf{T} to p dimensions. For more details, refer to Appendix A.

5 Experiments

Similar to the Word Tour experiments, we used 300-dimensional GloVe (Pennington et al., 2014) with $n = 40,000$, and the LKH solver⁵ (Helsgaun, 2018) as the TSP solver.

For ICA, we employed FastICA (Hyvärinen, 1999) from scikit-learn (Pedregosa et al., 2011), setting iterations to 10,000 and tolerance to 10^{-10} , consistent with the setting in Yamagiwa et al. (2023). We computed the axis embeddings \mathbf{v}_ℓ in (3) with $k = 100$. For baselines, we used whitened PCA-transformed embeddings⁶, along with two

³The first $d\%p$ intervals are $\lfloor d/p \rfloor + 1$ in length, and the rest are $\lfloor d/p \rfloor$ in length, where $\lfloor \cdot \rfloor$ is the floor function.

⁴Since the skewness of the axis of \mathbf{S} is positive, $\gamma_\ell \geq 0$.

⁵The LKH solver is an implementation of Lin-Kernighan algorithm (Lin and Kernighan, 1973; Helsgaun, 2000).

⁶Whitened ICA-transformed embeddings are obtained by applying an orthogonal matrix to these embeddings.

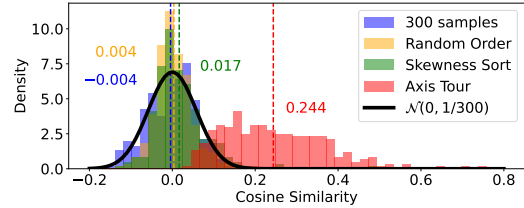


Figure 2: Histogram of the cosine similarity between consecutive axis embeddings $\cos(\mathbf{v}_i, \mathbf{v}_{i+1})$. As an additional baseline, we sampled 300 random words, ordered them, and showed the histogram of adjacent cosine similarities. The dashed lines indicates the average similarity for each method. The distribution for Axis Tour shifts towards a more positive mean, distancing itself from 0. Conversely, other distributions roughly follow the normal distribution with means that are close to 0.

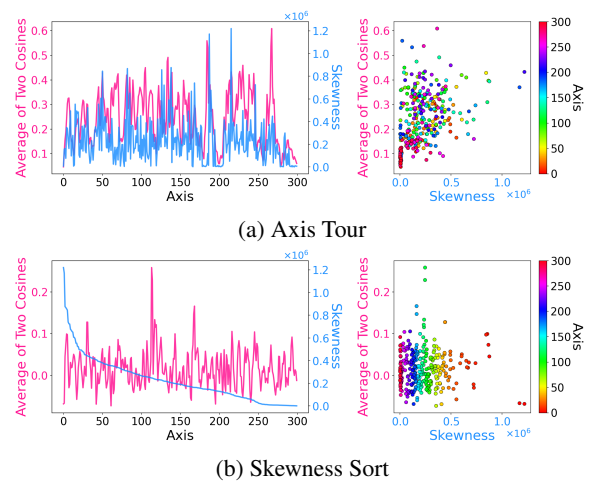


Figure 3: Relationship between the skewness and the average of consecutive two cosines (i.e., $(\cos(\mathbf{v}_{i-1}, \mathbf{v}_i) + \cos(\mathbf{v}_i, \mathbf{v}_{i+1}))/2$) for (a) Axis Tour and (b) Skewness Sort. The left shows the skewness and the average of two cosines for both y -axes, and the right shows the scatter plot of these values. Spearman’s rank correlation is 0.43 for Axis Tour, while it is 0.04 for Skewness Sort.

types of whitened ICA-transformed embeddings: **Random Order**, which randomizes the axes’ order in \mathbf{S} ⁷, and **Skewness Sort**, which arranges the axes of \mathbf{S} in descending order of skewness. See Appendix C for additional experiments.

5.1 Qualitative observation

Table 1 shows examples of consecutive axes extracted using Axis Tour. These examples demonstrate the semantic similarity between adjacent axes and illustrate how the meanings of the axes change continuously. For example, in top row, the axis meaning transition from *Eastern Europe* to *Ger-*

⁷In the embeddings matrix, we do not flip the sign of each axis to ensure positive skewness.

23	24	25	26	27	28	29	30	31
serb bosnian croatia croatian serbian	russian russia moscow sergei aleksandr	czech prague poland polish warsaw	germany german berlin von cologne	france french le paris du	canada canadian ontario quebec saskatchewan	australia australian queensland brisbane perth	wiltshire shrewsbury lincolnshire peterborough croydon	liga relegated fc f.c. serie
101	102	103	104	105	106	107	108	109
pay fees payments payment paid	land property lands estate bergisches	laws regulations enacted law provisions	court judge appellate appeals supreme	lawsuits lawsuit litigation suits suit	charges alleged prosecutors indicted convicted	camp prison buchenwald camps inmates	corpses corpse exhumed dismembered bodies	remain remained stayed stubbornly stays
237	238	239	240	241	242	243	244	245
award awards awarded prize emmy	film films movie starring directed	superhero marvel spin-off superheroes characters	album albums band self-titled ep	piano violin cello percussion orchestral	paintings painting art sculpture watercolor	manuscript biographies pages book handwritten	language languages pashto colloquial dialect	name names surname phrase misspelling

Table 1: Semantic continuity of axes via Axis Tour for normalized ICA-transformed embeddings. We apply Axis Tour to 300-dimensional GloVe and extract nine consecutive axes, then display the top five words for each axis.

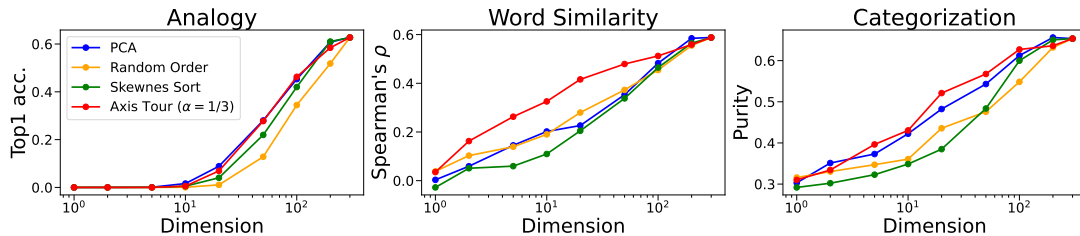


Figure 4: Dimensionality reduction performance for embeddings. Each value represents the average of 30 analogy tasks, 8 word similarity tasks, or 6 categorization tasks. For detailed experimental results, refer to Appendix B.

many and *France*, followed by *Canada* (which shares a connection with France) then to *Australia* (English-speaking regions), *the regions in England*, and finally to *soccer* (a popular sport in England), showcasing geographic and cultural continuity.

5.2 Cosine similarity between adjacent axis embeddings

Fig. 2 shows the histograms of $\cos(\mathbf{v}_i, \mathbf{v}_{i+1})$ for Axis Tour and the baselines. In Axis Tour, the values of $\cos(\mathbf{v}_i, \mathbf{v}_{i+1})$ are consistently higher, while this trend is not observed in the other baselines. This result is consistent with the formulation in (4).

For Axis Tour and Skewness Sort, Fig. 3 illustrates the relationship between the skewness and the average of the two adjacent cosine similarities⁸. In Fig. 3a for Axis Tour, it is interesting to note that these two values are correlated. However, no such trend is observed in Fig. 3b for Skewness Sort. This indicates that in Axis Tour, the axes with higher skewness are more likely to be ordered adjacent to the axes with higher similarity.

⁸Cosine similarity is not defined for the i -th axis itself.

5.3 Dimensionality reduction: analogy, word similarity, and categorization tasks

Using Word Embedding Benchmark (Jastrzebski et al., 2017)⁹, we evaluated dimensionality reduction performance in analogy, word similarity, and categorization tasks. PCA selects the axes in descending order of eigenvalue. Random Order and Skewness Sort select the axes sequentially from 1. Axis Tour applies the dimensionality reduction method in Section 4.3 with $\alpha = 1/3$ ¹⁰.

Fig. 4 shows that the dimensionality reduction for Axis Tour is better than or equal to the baselines for most dimensions in each task. This result suggests that the dimensionality reduction for Axis Tour efficiently merges the axes with similar meanings. For more details, refer to Appendix B.

6 Conclusion

In this study, we propose a novel method, Axis Tour, which optimizes the order of axes in ICA-transformed word embeddings. We focus on the fact that the word embeddings reveal interpretable

⁹<https://github.com/kudkudak/word-embeddings-benchmarks>.

¹⁰Fig. 6 in Appendix C.1 shows the results for different α .

semantic axes while the order of these axes are arbitrary. Axis Tour aims to improve the clarity of the word embedding space by maximizing the semantic continuity of the axes. Furthermore, we show through experiments on downstream tasks that Axis Tour constructs better low-dimensional embeddings compared to both PCA and ICA.

Limitations

- While the dimension reduction experiments showed the improvement of the downstream task performance for the Axis Tour embeddings, there are three aspects that could be further improved:
 1. Dimension reduction is performed using the vector \mathbf{f}_r , but its definition (5) is empirical, and better vectors may be designed. In addition, nonlinear transformations beyond linear ones could be considered for dimension reduction. Details on the definition of \mathbf{f}_r can be found in Appendix A.
 2. The method in Section 4.3 simply divides $[d]$ into p equal intervals to merge the axes. However, adaptively determining the division points could allow selecting more semantically coherent groups of axes.
 3. To construct optimal low-dimensional vectors using ICA-transformed embeddings, applying clustering methods such as K-means to axis embeddings may improve performance. In this case, the overall optimized axis order may not be determined as in Axis Tour, but performing Axis Tour within each cluster and then concatenating these could determine an axis order depending on the number of clusters.

However, this study focuses on a method for maximizing the semantic continuity of axes in ICA-transformed embeddings, leaving detailed investigation of the effective low-dimensional vector as future work.

- In Axis Tour, while adjacent axes may have similar meanings, axes with similar meanings may not be in close order. This is due to the fact that in Word Tour, high-dimensional embeddings result in one-dimensional embeddings, and the meanings of words are similar

when the word order is close, but semantically similar words are not always embedded close to each other.

- As seen in Fig. 1, projecting multiple axes of ICA-transformed embeddings into two dimensions can effectively represent the shape of the embeddings. However, as the number of axes increases, the angles between the axes become small, resulting in crowded axes. This can cause problems such as the top words of the axes being closer to the origin, which can be difficult to interpret.
- In Axis Tour, the dimension of the ICA-transformed embeddings corresponds to the number of cities in TSP. Therefore, as the dimension of the embeddings increases, the computation time for Axis Tour becomes longer. Note that for the 300-dimensional GloVe used in this study, the computation time for Axis Tour is about one second. For reference, Word Tour with $n = 40,000$ is known to take several hours¹¹.

Ethics Statement

This study complies with the [ACL Ethics Policy](#).

Acknowledgements

We would like to thank Momose Oyama for the discussion. This work was supported by JST, the establishment of university fellowships towards the creation of science technology innovation, Grant Number JPMJFS2123. This study was partially supported by JSPS KAKENHI 22H05106, 23H03355, JST CREST JPMJCR21N3.

References

- Abdulrahman Almuhareb and Massimo Poesio. 2005. [Concept learning and categorization from the web](#). *Proceedings of the Annual Meeting of the Cognitive Science Society*, 27.
- Marco Baroni, Stefan Evert, and Alessandro Lenci, editors. 2008. *Proceedings of the ESSLLI Workshop on Distributional Lexical Semantics: Bridging the Gap between Semantic Theory and Computational Simulations*. European Summer School in Logic, Language and Information (ESSLLI), Hamburg, Germany.

¹¹<https://github.com/joisino/wordtour>.

- Marco Baroni and Alessandro Lenci. 2011. [How we blessed distributional semantic evaluation](#). In *Proceedings of the GEMS 2011 Workshop on GEometrical Models of Natural Language Semantics, Edinburgh, UK, July 31, 2011*, pages 1–10. Association for Computational Linguistics.
- William F. Battig and William E. Montague. 1969. [Category norms of verbal items in 56 categories: A replication and extension of the connecticut category norms](#). *Journal of Experimental Psychology*, 80(3, Pt.2):1–46.
- Michael W Browne. 2001. An overview of analytic rotation in exploratory factor analysis. *Multivariate behavioral research*, 36(1):111–150.
- Elia Bruni, Nam-Khanh Tran, and Marco Baroni. 2014. Multimodal distributional semantics. *Journal of Artificial Intelligence Research*, 49:1–47.
- Charles B Crawford and George A Ferguson. 1970. A general rotation criterion and its use in orthogonal rotation. *Psychometrika*, 35(3):321–332.
- Hoagy Cunningham, Aidan Ewart, Logan Riggs, Robert Huben, and Lee Sharkey. 2023. [Sparse autoencoders find highly interpretable features in language models](#). *CoRR*, abs/2309.08600.
- Lev Finkelstein, Evgeniy Gabrilovich, Yossi Matias, Ehud Rivlin, Zach Solan, Gadi Wolfman, and Eytan Ruppín. 2002. Placing search in context: The concept revisited. *ACM Transactions on information systems*, 20(1):116–131.
- Keld Helsgaun. 2000. [An effective implementation of the lin-kernighan traveling salesman heuristic](#). *Eur. J. Oper. Res.*, 126(1):106–130.
- Keld Helsgaun. 2018. [LKH \(Keld Helsgaun\)](#).
- Felix Hill, Roi Reichart, and Anna Korhonen. 2015. Simlex-999: Evaluating semantic models with (genuine) similarity estimation. *Computational Linguistics*, 41(4):665–695.
- Aapo Hyvärinen. 1999. [Fast and robust fixed-point algorithms for independent component analysis](#). *IEEE Trans. Neural Networks*, 10(3):626–634.
- Aapo Hyvärinen, Patrik O. Hoyer, and Mika Inki. 2001a. [Topographic independent component analysis](#). *Neural Comput.*, 13(7):1527–1558.
- Aapo Hyvärinen, Juha Karhunen, and Erkki Oja. 2001b. [Independent Component Analysis](#). Wiley.
- Aapo Hyvärinen and Erkki Oja. 2000. [Independent component analysis: algorithms and applications](#). *Neural Networks*, 13(4-5):411–430.
- Stanislaw Jastrzebski, Damian Lesniak, and Wojciech Marian Czarnecki. 2017. [How to evaluate word embeddings? on importance of data efficiency and simple supervised tasks](#). *CoRR*, abs/1702.02170.
- Teuvo Kohonen. 2001. *Self-Organizing Maps, Third Edition*. Springer Series in Information Sciences. Springer.
- Shen Lin and Brian W. Kernighan. 1973. [An effective heuristic algorithm for the traveling-salesman problem](#). *Oper. Res.*, 21(2):498–516.
- Thang Luong, Richard Socher, and Christopher Manning. 2013. Better word representations with recursive neural networks for morphology. In *Proceedings of the Seventeenth Conference on Computational Natural Language Learning*, pages 104–113.
- David Mareček, Jindřich Libovický, Tomáš Musil, Rudolf Rosa, and Tomasz Limisiewicz. 2020. *Hidden in the Layers: Interpretation of Neural Networks for Natural Language Processing*, volume 20 of *Studies in Computational and Theoretical Linguistics*. Institute of Formal and Applied Linguistics, Prague, Czechia.
- Tomás Mikolov, Kai Chen, Greg Corrado, and Jeffrey Dean. 2013a. [Efficient estimation of word representations in vector space](#). In *1st International Conference on Learning Representations, ICLR 2013, Scottsdale, Arizona, USA, May 2-4, 2013, Workshop Track Proceedings*.
- Tomás Mikolov, Wen-tau Yih, and Geoffrey Zweig. 2013b. [Linguistic regularities in continuous space word representations](#). In *Human Language Technologies: Conference of the North American Chapter of the Association of Computational Linguistics, Proceedings, June 9-14, 2013, Westin Peachtree Plaza Hotel, Atlanta, Georgia, USA*, pages 746–751. The Association for Computational Linguistics.
- Tomás Musil. 2019. [Examining structure of word embeddings with PCA](#). In *Text, Speech, and Dialogue - 22nd International Conference, TSD 2019, Ljubljana, Slovenia, September 11-13, 2019, Proceedings*, volume 11697 of *Lecture Notes in Computer Science*, pages 211–223. Springer.
- Tomás Musil and David Marecek. 2022. [Independent components of word embeddings represent semantic features](#). *CoRR*, abs/2212.09580.
- Sungjoon Park, JinYeong Bak, and Alice Oh. 2017. [Rotated word vector representations and their interpretability](#). In *Proceedings of the 2017 Conference on Empirical Methods in Natural Language Processing, EMNLP 2017, Copenhagen, Denmark, September 9-11, 2017*, pages 401–411. Association for Computational Linguistics.
- Fabian Pedregosa, Gaël Varoquaux, Alexandre Gramfort, Vincent Michel, Bertrand Thirion, Olivier Grisel, Mathieu Blondel, Peter Prettenhofer, Ron Weiss, Vincent Dubourg, Jake VanderPlas, Alexandre Passos, David Cournapeau, Matthieu Brucher, Matthieu Perrot, and Edouard Duchesnay. 2011. [Scikit-learn: Machine learning in python](#). *J. Mach. Learn. Res.*, 12:2825–2830.

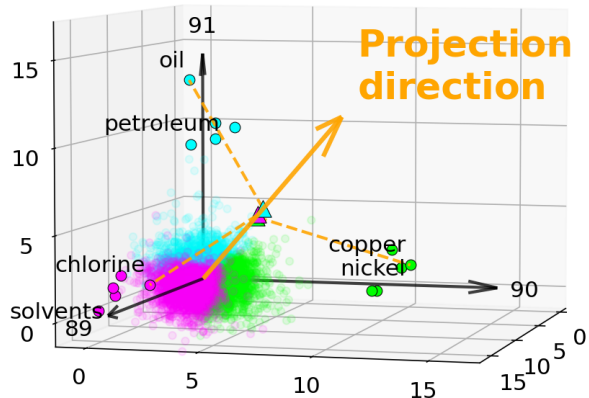


Figure 5: Projection of the subspace spanned by three consecutive axes in Fig. 1 into a one-dimensional space. Each word is assigned the color of the axis with the highest value. The projection direction is in the direction representing the subspace. For visualization, we randomly sampled 10,000 words, excluding the top 5 words on each axis.

Jeffrey Pennington, Richard Socher, and Christopher D. Manning. 2014. [Glove: Global vectors for word representation](#). In *Proceedings of the 2014 Conference on Empirical Methods in Natural Language Processing, EMNLP 2014, October 25-29, 2014, Doha, Qatar, A meeting of SIGDAT, a Special Interest Group of the ACL*, pages 1532–1543. ACL.

Kira Radinsky, Eugene Agichtein, Evgeniy Gabrilovich, and Shaul Markovitch. 2011. A word at a time: Computing word relatedness using temporal semantic analysis. In *Proceedings of the 20th International Conference on World Wide Web*, page 337–346.

Herbert Rubenstein and John B. Goodenough. 1965. [Contextual correlates of synonymy](#). *Commun. ACM*, 8(10):627–633.

Ryoma Sato. 2022. [Word tour: One-dimensional word embeddings via the traveling salesman problem](#). In *Proceedings of the 2022 Conference of the North American Chapter of the Association for Computational Linguistics: Human Language Technologies, NAACL 2022, Seattle, WA, United States, July 10-15, 2022*, pages 2166–2172. Association for Computational Linguistics.

Hiroaki Yamagiwa, Momose Oyama, and Hidetoshi Shimodaira. 2023. [Discovering universal geometry in embeddings with ICA](#). In *Proceedings of the 2023 Conference on Empirical Methods in Natural Language Processing, EMNLP 2023, Singapore, December 6-10, 2023*, pages 4647–4675. Association for Computational Linguistics.

A Dimensionality reduction

This section details and supplements Section 4.3.

A.1 Definition of \mathbf{f}_r

Here we first discuss the definition of \mathbf{f}_r in terms of skewness and then explain the normalization.

Skewness as weight. In (3), a vector $\mathbf{f}_r = (f_r^{(\ell)})_{\ell=1}^d \in \mathbb{R}_{\geq 0}^d$ for dimensionality reduction is defined by the skewness $\gamma_\ell \in \mathbb{R}_{\geq 0}$ of the ℓ -th axis of \mathbf{T} . In particular, $f_r^{(\ell)}$, which corresponds to the weight of the ℓ -th axis in the projection, is proportional to γ_ℓ^α ($\alpha \in \mathbb{R}_{\geq 0}$). This is based on the assumption that the axis becomes more meaningful as the skewness increases¹². Higher-order statistics such as skewness are known to be sensitive to outliers (Hyvärinen et al., 2001b), so we mitigate this effect by raising γ_ℓ to the power of α . Since skewness is a third-order moment, we treat $\alpha = 1/3$ as the default value. $\alpha = 0$ is a uniform weight, while $\alpha = 1$ is the original γ_ℓ . Next, we will explain why \mathbf{f}_r is normalized.

Reason for Normalizing \mathbf{f}_r . \mathbf{f}_r is normalized (i.e., $\|\mathbf{f}_r\| = 1$) to equalize the scale of the one-dimensional projections for each subspace. Thus, when $p = d$, $\mathbf{TF} = \mathbf{T}$ holds.

For $p = d$, $I_r = \{r\}$, and from (3), $\mathbf{f}_r = (f_r^{(\ell)})_{\ell=1}^d$ satisfies:

$$f_r^{(\ell)} = \delta_{\ell r} = \begin{cases} 1 & \ell = r \\ 0 & \ell \neq r \end{cases}. \quad (6)$$

Here, $\delta_{\ell r}$ is the Dirac delta function. From (6) the matrix $\mathbf{F} = [\mathbf{f}_1, \dots, \mathbf{f}_d] \in \mathbb{R}^{d \times d}$ corresponds to the d -dimensional identity matrix $\mathbf{I} \in \mathbb{R}^{d \times d}$, so $\mathbf{TF} = \mathbf{TI} = \mathbf{T}$.

A.2 Projection from subspace to one-dimensional space

This section explains the projection from a subspace to a one-dimensional space using a specific example. Consider the subspace spanned by three consecutive axes (89, 90, 91) from Fig. 1. Fig. 5 shows the projection of this subspace using \mathbf{f}_r . The projection direction is in the direction representing the subspace, and the top words of each axis are projected close together.

B Details of experiment in Section 5

The embedding of the word w_i is denoted by $\mathbf{w}_i \in \mathbb{R}^d$.

¹²While not specific to ICA-transformed embeddings, it is known from a study of sparse coding for language models that skewness correlates with interpretability (Cunningham et al., 2023).

Tasks	$p = 5$				$p = 20$				$p = 100$				$p = 300$
	PCA	Rand.	Skew.	Tour.	PCA	Rand.	Skew.	Tour.	PCA	Rand.	Skew.	Tour.	All
capital-common-countries	0.00	0.00	0.00	0.00	0.37	0.00	0.06	0.11	0.95	0.56	0.85	0.87	0.95
capital-world	0.00	0.00	0.00	0.00	0.26	0.02	0.05	0.11	0.90	0.73	0.80	0.82	0.95
city-in-state	0.00	0.00	0.00	0.00	0.03	0.00	0.02	0.04	0.42	0.28	0.24	0.40	0.67
currency	0.00	0.00	0.00	0.00	0.02	0.00	0.00	0.02	0.09	0.08	0.08	0.10	0.12
family	0.01	0.00	0.00	0.00	0.40	0.02	0.08	0.22	0.78	0.68	0.80	0.75	0.88
gram1-adjective-to-adverb	0.00	0.00	0.00	0.00	0.01	0.00	0.01	0.01	0.08	0.08	0.14	0.09	0.21
gram2-opposite	0.00	0.00	0.00	0.00	0.00	0.00	0.00	0.00	0.14	0.12	0.18	0.14	0.26
gram3-comparative	0.00	0.00	0.00	0.00	0.05	0.01	0.04	0.11	0.62	0.46	0.58	0.66	0.88
gram4-superlative	0.00	0.00	0.00	0.00	0.01	0.00	0.00	0.01	0.31	0.54	0.23	0.31	0.69
gram5-present-participle	0.00	0.00	0.00	0.00	0.03	0.00	0.03	0.07	0.44	0.30	0.59	0.58	0.69
gram6-nationality-adjective	0.00	0.00	0.00	0.00	0.57	0.07	0.22	0.43	0.91	0.88	0.91	0.88	0.93
gram7-past-tense	0.00	0.00	0.00	0.00	0.05	0.02	0.04	0.06	0.45	0.36	0.47	0.51	0.60
gram8-plural	0.00	0.00	0.00	0.00	0.11	0.01	0.04	0.07	0.73	0.40	0.59	0.56	0.76
gram9-plural-verbs	0.00	0.00	0.00	0.00	0.06	0.01	0.02	0.06	0.39	0.27	0.29	0.53	0.58
jj_jjr	0.00	0.00	0.00	0.00	0.01	0.00	0.01	0.03	0.35	0.23	0.29	0.43	0.66
jj_jjs	0.00	0.00	0.00	0.00	0.01	0.00	0.00	0.01	0.21	0.36	0.14	0.20	0.51
jjr_ij	0.00	0.00	0.00	0.00	0.01	0.00	0.03	0.02	0.33	0.27	0.32	0.33	0.54
jjr_jjs	0.00	0.00	0.00	0.00	0.01	0.00	0.01	0.01	0.24	0.37	0.15	0.20	0.55
jjs_ij	0.00	0.00	0.00	0.00	0.01	0.00	0.01	0.01	0.21	0.13	0.18	0.19	0.48
jjs_jjr	0.00	0.00	0.00	0.00	0.01	0.00	0.01	0.01	0.29	0.16	0.25	0.33	0.63
nn_nnpos	0.00	0.00	0.00	0.00	0.05	0.01	0.01	0.04	0.35	0.20	0.29	0.28	0.42
nn_nns	0.00	0.00	0.00	0.00	0.04	0.00	0.04	0.06	0.55	0.33	0.49	0.51	0.74
nnpos_nn	0.00	0.00	0.00	0.00	0.03	0.00	0.02	0.06	0.40	0.20	0.34	0.31	0.45
nns_nn	0.00	0.00	0.00	0.00	0.05	0.00	0.04	0.06	0.48	0.30	0.43	0.44	0.64
vb_vbd	0.00	0.00	0.00	0.00	0.11	0.03	0.09	0.07	0.45	0.36	0.40	0.54	0.58
vb_vbz	0.00	0.00	0.00	0.00	0.09	0.02	0.05	0.08	0.58	0.33	0.50	0.68	0.76
vbd_vb	0.00	0.00	0.00	0.00	0.09	0.04	0.12	0.08	0.46	0.36	0.56	0.56	0.69
vbd_vbz	0.00	0.00	0.00	0.00	0.08	0.01	0.04	0.05	0.48	0.26	0.38	0.54	0.63
vbz_vb	0.00	0.00	0.00	0.00	0.06	0.02	0.06	0.11	0.65	0.43	0.70	0.70	0.82
vbz_vbd	0.00	0.00	0.00	0.00	0.05	0.01	0.03	0.05	0.33	0.33	0.42	0.44	0.55
Average	0.00	0.00	0.00	0.00	0.09	0.01	0.04	0.07	0.45	0.34	0.42	0.46	0.63
MEN	0.16	0.19	0.11	0.35	0.32	0.33	0.29	0.51	0.66	0.56	0.63	0.66	0.75
MTurk	0.17	0.08	0.12	0.32	0.38	0.32	0.30	0.52	0.57	0.53	0.57	0.61	0.64
RG65	0.31	0.09	0.05	0.29	0.36	0.42	0.28	0.50	0.68	0.66	0.59	0.63	0.78
RW	0.09	0.10	0.07	0.13	0.14	0.16	0.10	0.25	0.24	0.32	0.28	0.30	0.34
SimLex999	0.01	0.13	0.04	0.07	0.11	0.21	0.08	0.21	0.27	0.37	0.28	0.31	0.40
WS353	0.12	0.16	0.02	0.31	0.15	0.28	0.18	0.44	0.47	0.40	0.43	0.52	0.57
WS353R	0.12	0.14	0.01	0.17	0.15	0.16	0.15	0.35	0.40	0.28	0.35	0.44	0.51
WS353S	0.18	0.21	0.06	0.45	0.21	0.35	0.26	0.55	0.57	0.51	0.58	0.62	0.69
Average	0.15	0.14	0.06	0.26	0.23	0.28	0.20	0.42	0.48	0.45	0.46	0.51	0.59
AP	0.33	0.22	0.22	0.27	0.36	0.26	0.28	0.40	0.51	0.45	0.54	0.56	0.66
BLESS	0.31	0.28	0.27	0.36	0.42	0.36	0.35	0.51	0.73	0.68	0.69	0.76	0.79
Battig	0.18	0.10	0.12	0.15	0.24	0.14	0.16	0.22	0.37	0.29	0.35	0.34	0.42
ESSLI_1a	0.50	0.41	0.45	0.64	0.61	0.57	0.48	0.77	0.73	0.59	0.73	0.75	0.70
ESSLI_2b	0.47	0.62	0.45	0.53	0.73	0.68	0.55	0.68	0.75	0.75	0.70	0.75	0.78
ESSLI_2c	0.44	0.44	0.42	0.44	0.53	0.60	0.49	0.56	0.58	0.53	0.60	0.60	0.58
Average	0.37	0.35	0.32	0.40	0.48	0.44	0.38	0.52	0.61	0.55	0.60	0.63	0.65

Table 2: Dimensionality reduction performance for p -dimensional embeddings. *Rand.* stands for Random Order, *Skew.* for Skewness Sort, and *Tour.* for Axis Tour. The values in the table correspond to top 1 accuracy for analogy tasks, Spearman’s rank correlation for word similarity tasks, and purity for categorization tasks. Note that at $p = 300$, all embeddings give the same results.

Analogy task. We used the Google Analogy Test Set (Mikolov et al., 2013a), which contains 14 types of analogy tasks, and the Microsoft Research Syntactic Analogies Dataset (Mikolov et al., 2013b), which contains 16 types of analogy tasks. In the analogy tasks, the quality of the embeddings is evaluated by inferring w_4 to which w_3 corresponds if w_1 corresponds to w_2 . We compute the vector $\mathbf{w}_2 - \mathbf{w}_1 + \mathbf{w}_3$ and see if the closest embedding is \mathbf{w}_4 (top1 accuracy).

Word similarity task. We used MEN (Bruni et al., 2014), MTurk (Radinsky et al., 2011), RG65 (Rubenstein and Goodenough, 1965), RW (Luong et al., 2013), SimLex999 (Hill et al., 2015), WS353 (Finkelstein et al., 2002), WS353R (WS353 Relatedness), and WS353S (WS353 Similarity). In the word similarity tasks, the quality of the embeddings is evaluated by measuring the cosine similarity of the word embeddings and comparing it to the human-rated similarity scores. As the evaluation metric, we used Spearman’s rank

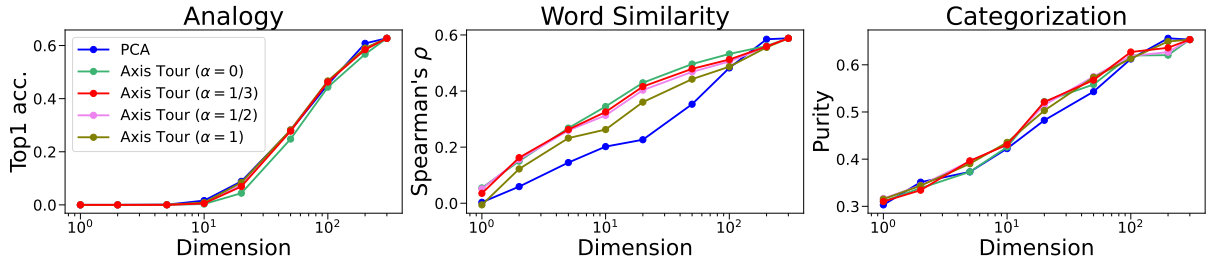


Figure 6: Dimensionality reduction performance for the PCA-transformed embeddings and the Axis Tour embeddings whose $\alpha = 0, 1/3, 1/2, 1$. Each value represents the average of 30 analogy tasks, 8 word similarity tasks, or 6 categorization tasks.

correlation coefficient between the human ratings and the cosine similarity.

Categorization task. We used AP (Almuhareb and Poesio, 2005), BLESS (Baroni and Lenci, 2011), Battig (Battig and Montague, 1969), ESSLLI_1a (Baroni et al., 2008), ESSLLI_2b (Baroni et al., 2008), and ESSLLI_2c (Baroni et al., 2008). In the categorization tasks, the quality of the embeddings is evaluated by clustering them in the setting where each word is assigned a class label. As the evaluation metric, we used Purity, which shows the proportion of the most frequent class in the clusters. As clustering methods, we used Hierarchical Clustering with five settings¹³ and K-means¹⁴, and then selected the one that gave the highest purity.

Results. Table 2 shows detailed experimental results of PCA, Random Order, Skewness Sort, and Axis Tour at $p = 5, 20, 100, 300$ for each task. As already seen, Fig. 4 in Section 5 shows the average of each task at $p = 1, 2, 5, 10, 20, 50, 100, 200, 300$ for the embeddings.

The Axis Tour embeddings showed superior performance in the word similarity tasks and the categorization tasks for almost all dimensions compared to other methods. In the analogy tasks, the Axis Tour embeddings achieved performance comparable to PCA and better than Random Order and Skewness Sort in most dimensions.

Note that the experimental results are the same for all embeddings for $p = 300$. First, as we saw in Appendix A.1, when $p = d (= 300)$, the matrix \mathbf{TF} (i.e., the projected p -dimensional embeddings)

¹³By default, Word Embedding Benchmark uses the following affinity and linkage pairs for hierarchical clustering: (affinity, linkage) = (euclidean, ward), (euclidean, average), (euclidean, complete), (cosine, average), (cosine, complete).

¹⁴We used the same seed for all experiments.

is equal to the matrix \mathbf{T} (i.e., the d -dimensional Axis Tour embeddings). Then, by definition, Axis Tour, Random Order, and Skewness Sort are the embeddings obtained by reordering the axes of the ICA-transformed embeddings and flipping their signs as needed. Thus, these three can be seen as the embeddings obtained by applying an orthogonal matrix to the ICA-transformed embeddings. Since the ICA-transformed embeddings are derived from the PCA-transformed embeddings by applying an orthogonal matrix¹⁵, cosine similarity and Euclidean distance remain unchanged for PCA, Random Order, Skewness Sort, and Axis Tour, leading to identical results in downstream tasks.

C Additional experiments

C.1 Comparison of α

Fig. 6 shows the average of each task at $p = 1, 2, 5, 10, 20, 50, 100, 200, 300$ for the PCA-transformed embeddings and the Axis Tour embeddings whose $\alpha = 0, 1/3, 1/2, 1$.

From Fig. 6, we can see that the performance of the Axis Tour embeddings changes for each task, depending on α . For example, when comparing across all α , while $\alpha = 1$ shows good performance on analogy tasks and poor performance on word similarity tasks, $\alpha = 0$ shows the opposite. These results indicate that the quality of low-dimensional embeddings by the Axis Tour embeddings depends on the vector \mathbf{f}_r for projection. However, the overall changes for each alpha are not as large, and in all tasks the performance is comparable to or better than that of the PCA-transformed embeddings, indicating the ability to construct high-quality low-dimensional embeddings.

¹⁵Refer to the previous work for the relationship between PCA and ICA (Yamagiwa et al., 2023).